Mn moment instability in the $TbMn_2$ intermetallic compound

1992 J. Phys.: Condens. Matter 4 1103

(http://iopscience.iop.org/0953-8984/4/4/020)

J. Phys.: Condens. Matter 4 (1992) 1103–1113. Printed in the UK

Mn moment instability in the $TbMn_2$ intermetallic compound

P J Brown†, B Ouladdiaf†, R Ballou‡, J Deportes‡ and A S Markosyan§

† Institut Laue–Langevin, 156X, 38042 Grenoble Cédex, France

‡ Laboratoire L. Néel, CNRS, 166X, Grenoble Cédex, France

§ Department of Physics, M V Lomonosov Moscow State University, Leninskie Gory, 119899 Moscow, USSR

Received 8 August 1991, in final form 30 September 1991

Abstract. Neutron diffraction experiments have been performed on a $TbMn_2$ single crystal and on $Tb(Mn_{0.96}Fe_{0.04})_2$ powder samples. The magnetic structure of $TbMn_2$ is metastable poised between two structures, S_1 with propagation vector $[\frac{2}{3}\frac{2}{3}0]$ and S_2 with propagation vector $[\frac{1}{2}\frac{1}{2}\frac{1}{2}]$. A transition from S_1 to S_2 can be induced either by an applied field of 4.5 T at 25 K or by chemical pressure induced by substitution of Mn by Fe. The S_2 structure has been studied in $Tb(Mn_{0.96}Fe_{0.04})_2$. The transition to this structure is accompanied by a huge rhombohedral distortion and the structure itself is notable for the coexistence of magnetic and non-magnetic manganese atoms. This peculiar feature is attributed to instability of the Mn moment combined with frustration of the Mn itinerant antiferromagnetism.

1. Introduction

The Laves phases RMn_2, where R ≡ rare earth, Y and Th, exhibit a wealth of original magnetic behaviour associated with the onset of itinerant antiferromagnetism in frustrated lattices. When the Mn moment is close to instability, the magnetism becomes complex and presents exotic features. The unusual properties of RMn_2 compounds have attracted much attention and have been investigated using various techniques both macroscopic methods (such as magnetization and thermal expansion measurements) and microscopic techniques (e.g. neutron and x-ray diffraction and NMR measurements).

Depending on the rare earth, the RMn_2 compounds crystallize either in the cubic FCC Laves phase (C15) with R ≡ Y, Gd, Tb, Dy or the hexagonal Laves phase (C14) when R ≡ Pr, Nd, Er, Lu, Th. $HoMn_2$ and $SmMn_2$ are dimorphic, the structure obtained depending upon the heat treatment. The Mn atoms lie at the vertices of regular tetrahedra. These tetrahedra are stacked in chains along the sixfold axis in the hexagonal phase and they are packed in the diamond arrangement, connected by sharing vertices in the cubic structure. In both structures, the topology of the packing ensures that any antiferromagnetic ordering will be highly frustrated.

Recent studies have shown that the Mn magnetism in these compounds is close to an instability which can give huge magnetovolumic anomalies (Wada *et al* 1987b). The occurrence of these anomalies depends on the Mn–Mn interatomic distances (Shiga 1988). There is a critical distance (d_c = 2.66 Å) below which the Mn moment is unstable. When the Mn–Mn distance is significantly lower than d_c as in $ErMn_2$, Mn is

0953-8984/92/041103+11$04.50

non-magnetic and the compound exhibits ferromagnetic ordering characteristic of the rare earth moments only (Felcher *et al* 1965). When the Mn–Mn interatomic distance is just below d_c as in $HoMn_2$ and $DyMn_2$, Mn magnetism is induced by cooperative exchange interactions but no magnetovolume effects are observed (Chamberlain 1977, Yoshimura *et al* 1986a,b). The value of the induced Mn moment is $1.4\mu_B$. When the Mn–Mn spacing is greater than d_c as in $NdMn_2$ and $PrMn_2$ (Ballou *et al* 1988), the Mn magnetism is well stabilized and Mn ordering is accompanied by a large magnetovolume effect. Unusual magnetic structures are found owing to the topological frustration. The value of the Mn moment is higher and can reach $2.7\mu_B$.

The critical spacing for the stability of Mn moments is probably that found in YMn_2 and $TbMn_2$, where the magnetovolume effects associated with the Mn moment instability is a maximum reaching 5% in YMn_2 and 1.5% in $TbMn_2$. The magnetic structure of YMn_2 is helimagnetic with a long period (280 Å) and distorted by the Mn magnetic anisotropy (Ballou *et al* 1987). The magnetic structure of $TbMn_2$ is more complex and not yet fully determined. In early work, Corliss and Hastings (1964) suggested a helimagnetic structure with a period of 8 Å, but owing to the poor resolution of their pattern they could not confirm this structure.

Because of the Mn instability, the magnetic properties of $TbMn_2$ and YMn_2 are very sensitive to external parameters such as applied pressure, applied magnetic field (Ballou *et al* 1991a) or the chemical pressure induced by alloying. The variation in the Néel temperature with hydrostatic pressure reaches -36 K kbar^{-1} in YMn_2 and $TbMn_2$ (Voiron *et al* 1990). A very small substitution of Mn by other 3d metals Fe, Co and Al (Yoshimura *et al* 1986b) or of Tb or Y by Lu or Sc (Wada *et al* 1987a, Levetin *et al* 1988) abruptly destabilizes the Mn ordering. The instability is also apparent from the lack of moment on some Mn sites in $DyMn_2$ (Yoshimura *et al* 1986a) and $ThMn_2$ (Deportes *et al* 1987). In order to get a clear insight into the magnetic state of Mn in $TbMn_2$, we have performed a neutron diffraction experiment on a $TbMn_2$ single crystal. We have also studied the magnetic properties of the $Tb(Mn_{1-x}Fe_x)_2$ system, in which a rapid loss of Mn magnetism associated with Fe substitution was expected, with neutron and x-ray diffraction. The x-ray studies of the crystal structure and magnetization in the 8–300 K temperature range (Ballou *et al* 1991b) show that the magnetovolume effects associated with antiferromagnetic ordering of the Mn moments disappear for $x > 0.02$ as shown in figure 1. A negative deviation in the cell parameter $a(T)$ is observed for $0.02 \leqslant x \leqslant 0.05$, indicating a change in the magnetic structure of the $TbMn_2$ compound. In this paper we present the main results obtained from a single-crystal neutron diffraction study of a $TbMn_2$ sample and from neutron diffraction experiments on $Tb(Mn_{0.96}Fe_{0.04})_2$ polycrystalline samples.

2. Experiments

The single crystal of $TbMn_2$ was prepared by the Czochralski method in a high-frequency induction furnace. A cylindrical sample of 2 mm diameter and 5 mm height was extracted from the ingot obtained and checked by x-ray and neutron Laue diffraction. The polycrystalline sample of $Tb(Mn_{0.96}Fe_{0.04})_2$ was prepared using the cold-crucible method again in a high-frequency induction furnace and annealed at 800 °C for 3 days. No foreign phase other than the C15 cubic structure was detected by x-ray analysis. The single-crystal neutron diffraction experiment was performed

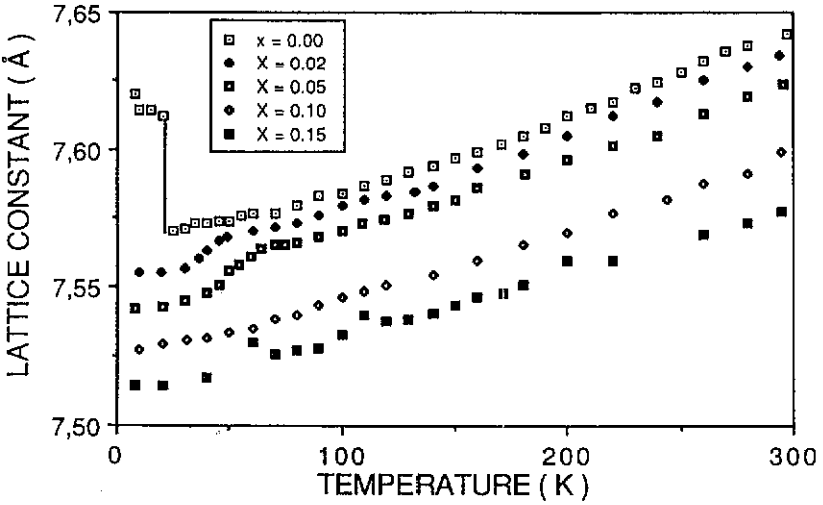

Figure 1. Thermal variation in lattice parameters for $Tb(Mn_{1-x}Fe_x)_2$ compounds from x-ray diffraction studies.

on the D15 diffractometer at the Institut Laue–Langevin (ILL) high-flux reactor in Grenoble. A cryomagnet was used for this experiment, giving a vertical field up to 6.5 T in the temperature range 1.5 to 300 K. The measurement was made using normal beam geometry with the twofold $[1\bar{1}0]$ axis of the crystal along the applied field. This configuration allows measurement of reflections of the form (hhl). The wavelength was $\lambda = 1.176$ Å. The powder neutron scattering was also made at ILL on the high-resolution neutron powder diffractometer D2B. The detectors of D2B cover a range of 160° in 2θ with a step width of $\delta(2\theta) = 0.05°$. The neutron wavelength was $\lambda = 1.594$ Å. The complete diffraction pattern was measured several times at each temperature to obtain good statistics. Measurements were performed in the temperature range from 5 to 120 K using a standard ILL 'orange' cryostat.

3. Results

3.1. Single-crystal studies on $TbMn_2$

When the sample is cooled in zero field, an increase in the intensities of the nuclear Bragg peaks is observed at 45 K, indicating a magnetic contribution to these peaks. Below 40 K, this magnetic contribution vanishes and the intensities of the nuclear reflections return to their high-temperature values. Below 40 K, additional peaks characteristic of antiferromagnetic ordering are detected. They can be indexed with a propagation vector $[\frac{2}{3}\frac{2}{3}0]$. A set of a small extra peaks is also observed, suggesting an incommensurate superstructure. At a very low temperature (2 K) a new set of magnetic peaks with small intensities is observed, in addition to the above magnetic peaks. The corresponding propagation vector is $[\frac{1}{2}\frac{1}{2}\frac{1}{2}]$. All these magnetic peaks are in agreement with those previously observed on powder samples.

When the sample is cooled in a field of 6.5 T, the magnetic contributions to the nuclear Bragg peaks observed at 45 K persist down to 2 K; their intensity increases with decreasing temperature to a saturation value at around 20 K. The magnetic

peaks associated with the $[\frac{2}{3}\frac{2}{3}0]$ propagation vector are still present but are weaker. In contrast the magnetic peaks generated by the $[\frac{1}{2}\frac{1}{2}\frac{1}{2}]$ propagation vector are strong and appear at around 40 K. Upon returning to zero field at 2 K these latter weaken drastically whereas the magnetic peaks generated by the $[\frac{2}{3}\frac{2}{3}0]$ propagation vector are strongly enhanced. A residual ferromagnetic component still persists even in zero field.

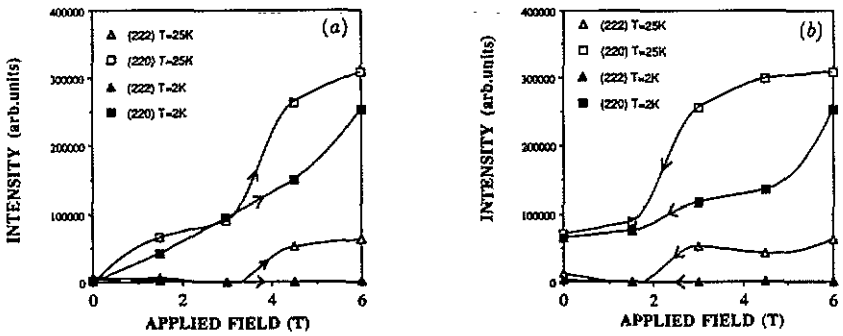

Figure 2. Neutron diffraction on $TbMn_2$ single crystal with $\lambda = 1.176$ Å, showing the field dependence of the ferromagnetic component ([000] propagation vector) at (222) and (220) peaks, measured at 2 and 25 K: (*a*) increasing field; (*b*) decreasing field.

Measurements in which the applied magnetic field was varied at fixed temperature have also been made after cooling in zero field from the paramagnetic phase to each required temperature. A particularity of the FCC Laves phase structure factors is that the intensity of the {222} peaks depends only on the Mn site nuclear scattering and ferromagnetic component, whereas that of the {220} peaks depends similarly on the Tb site only. The intensities of these two types of reflection give a direct measure of the evolution of the ferromagnetic component of Mn and Tb moments, respectively. Besides this, the intensity variation of the magnetic peaks indexed with $[\frac{2}{3}\frac{2}{3}0]$ and $[\frac{1}{2}\frac{1}{2}\frac{1}{2}]$ propagation vectors measures the stability with respect to the applied field of the magnetic structures (hereafter called S_1 and S_2, respectively) associated with each of these propagation vectors. We illustrate in figure 2, the variation at 2 K under an applied field in the intensities of the different peaks which characterize each magnetic contribution. The field dependence of the intensities of (220) and (222) (figure 2(*a*)) show clearly that a ferromagnetic alignment of the Tb moment is induced by fields greater than 3 T; however, no ferromagnetic alignment of the Mn moment is observed even in the highest available field (6.5 T). The intensity of the $(\frac{4}{3}\frac{4}{3}0)$ peak increases with increasing applied field, indicating a reinforcement of the magnetic structure S_1. In contrast the magnetic structure S_2 appears to be weakened (figure 3). Similar behaviour is observed at 25 K, up to $H_c = 4.5$ T, at which a field metamagnetic transition is observed. The intensity of the $(-\frac{3}{2} - \frac{3}{2}\frac{1}{2})$ reflection which characterizes S_2 increases gradually whereas the intensity of the $(\frac{4}{3}\frac{4}{3}0)$ reflection decreases, showing that S_2 is favoured above H_c to the detriment of S_1. The stabilization of S_2 is accompanied by the alignment of the ferromagnetic component of the Mn moment shown by the increase in the intensity of the (222) peak at 25 K. A large hysteresis with respect to the applied field is observed for these transitions (figures 2(*b*) and 3(*b*)).

It is clear from this study that the low-temperature magnetic state of $TbMn_2$ is a metastable multiphase state. This state consists mainly of the two magnetic structures

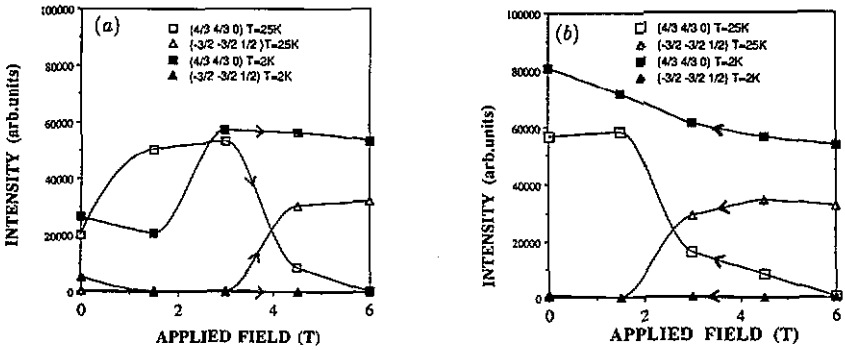

Figure 3. Neutron diffraction on $TbMn_2$ single crystal showing the field dependence of the antiferromagnetic components of propagation vectors $[\frac{2}{3}\frac{2}{3}0]$ and $[\frac{1}{2}\frac{1}{2}\frac{1}{2}]$ at $(\frac{4}{3}\frac{4}{3}0)$ and $(-\frac{3}{2}-\frac{3}{2}\frac{1}{2})$ peaks, respectively, measured at 2 and 25 K: (*a*) increasing field; (*b*) decreasing field.

S_1 and S_2 with propagation vectors $[\frac{2}{3}\frac{2}{3}0]$ and $[\frac{1}{2}\frac{1}{2}\frac{1}{2}]$, respectively, the latter being combined with a ferromagnetic component. The magnetic structure S_2 is stabilized with respect to S_1 under an applied magnetic field.

3.2. Powder neutron diffraction studies on $Tb(Mn_{0.96}Fe_{0.04})_2$

The powder diffraction pattern obtained at 120 K is shown in figure 4(*a*); it is characteristic of the nuclear Bragg reflections associated with the crystallographic $MgCu_2$ (C15)-type structure; only the reflections with h, k, l all even or all odd are observed. No extra lines are present. The refinement of the magnetic and nuclear structures at different temperatures was done using a Rietveld refinement method. The nuclear scattering lengths used in the calculation are $b_{Tb} = 0.738 \times 10^{-12}$ cm, $b_{Mn} = -0.373 \times 10^{-12}$ cm and $b_{Fe} = 0.954 \times 10^{-12}$ cm. In figure 4, the full curve represents the calculated pattern, the short vertical lines the experimental pattern and the lower curve shows the difference between the two. Good agreement is obtained. Below 90 K, the intensities of the Bragg peaks increase gradually with decreasing temperature (figure 4(*b*). The Rietveld refinement of the magnetic intensities shows that the increase corresponds to ferrimagnetic alignment of the Tb and Mn moments. Because of the averaging effect due to cubic symmetry, the direction of the moments cannot be determined. However, magnetization measurements on a single crystal (Ballou *et al* 1991b) have shown that the magnetization direction is [111]. Finally the width of the peaks at large angles are greater than that observed at 120 K, indicating a small crystallographic distortion.

Between 30 and 70 K, the intensity due to the ferrimagnetic contribution to the Bragg reflections increases and a progressive crystallographic distortion takes place, which results in the splitting of the Bragg reflections at large angles. The cubic cell is distorted by elongation along the [111] direction as is shown by the fact that the (444) peak splits into two peaks with an intensity ratio 1:3 and the (840) peak splits into two peaks with equal intensities. This is characteristic of a crystallographic distortion from cubic to rhombohedral. Figure 5 shows the shape of the (444) peak at 120, 30 and 5 K.

Below 30 K (figure 4(*c*)), the patterns are characterized by the presence of extra peaks, which can be indexed with the propagation vector $[\frac{1}{2}\frac{1}{2}\frac{1}{2}]$, in addition to the ferrimagnetic and nuclear Bragg reflections. They are characteristic of antiferromag-

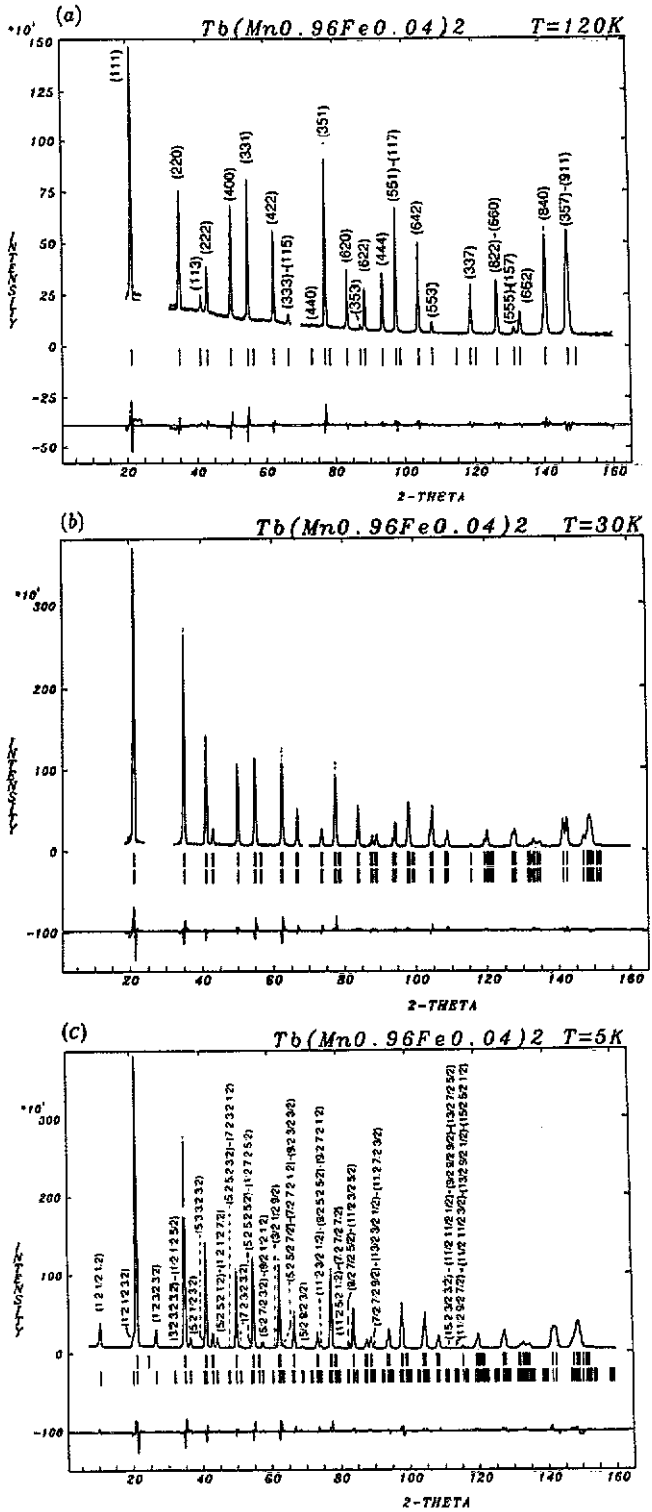

Figure 4. $Tb(Mn_{0.96}Fe_{0.04})_2$ powder neutron diffraction patterns with $\lambda = 1.594$ Å at (*a*) $T = 120$ K, (*b*) $T = 30$ K and (*c*) $T = 5$ K. The full curves are the calculated data, and the lower curves show the difference between observation and calculation.

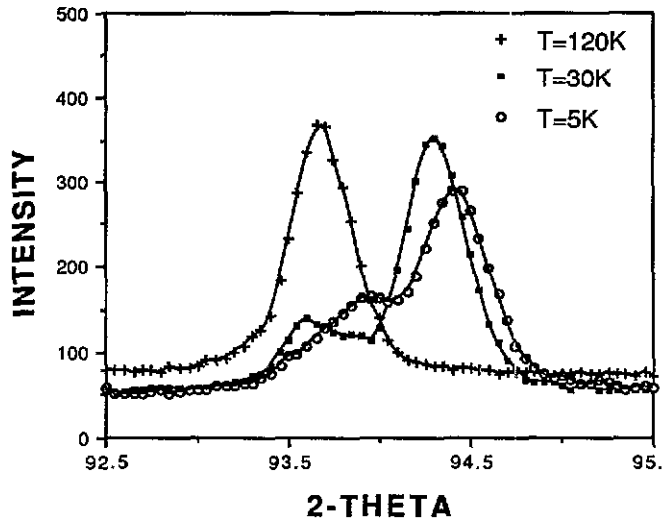

Figure 5. The shape of (444) peak at 120, 30 and 5 K obtained from powder neutron diffraction on $Tb(Mn_{0.96}Fe_{0.04})_2$.

netic order similar to the magnetic structure S_2 of $TbMn_2$. Their intensities increase with decreasing temperature; the magnetic cell is then eight times larger than the crystallographic cell. The analysis of the magnetic structure factors of the antiferrimagnetic peaks and especially the fact that $(\frac{1}{2}\frac{1}{2}\frac{1}{2})$ is relatively stronger than $(\frac{3}{2}\frac{3}{2}\frac{3}{2})$, $(\frac{5}{2}\frac{1}{2}\frac{1}{2})$ requires that the Tb atoms at $(\frac{1}{8},\frac{1}{8},\frac{1}{8})$ and $(-\frac{1}{8},-\frac{1}{8},-\frac{1}{8})$ be coupled antiferromagnetically, parallel and antiparallel respectively to the Mn moment at $(\frac{1}{2},\frac{1}{2},\frac{1}{2})$, implying that the centre of symmetry at the origin is combined with time inversion. The resulting structure consists of ferrimagnetic planes of Mn and Tb atoms with moments inclined at about 25° to the [111] axis. The components of moments perpendicular to [111] in successive layers are antiparallel and there is a layer of weakly magnetic Mn atoms between each strongly magnetic Tb–Mn layer. This time inversion symmetry together with the propagation vector $[\frac{1}{2}\frac{1}{2}\frac{1}{2}]$ is not consistent with the existence of moment on the other three Mn sublattices, which are at the centres of symmetry and which, like that at the origin, are combined with time-reversal. The magnetic structure obtained can be described by a component of moment parallel to [111] with propagation vector [000] with ferrimagnetic coupling of Tb and Mn combined with an antiferromagnetic component in the (111) planes with propagation vector $[\frac{1}{2}\frac{1}{2}\frac{1}{2}]$. For this latter, the moments in a given (111) plane are parallel to one another but adjacent (111) planes are antiparallel. This type of antiferromagnetic ordering is observed in MnO (Bertaut 1972) and $DyMn_2$ (Ritter *et al* 1991); however, no crystallographic distortion was observed in $DyMn_2$ owing to the limitation in the scattering angle. From figure 5 we can see that the splitting of the (444) peaks at 5 K is lower than at 30 K, indicating a decrease in the rhombohedral distortion when antiferromagnetic order sets in. We have reported in figure 6 the thermal variation in the distortion parameter ϵ with $\epsilon = 90 - \alpha_R$, where a_R and α_R are the rhombohedral lattice parameters. a_R exhibits a small deviation from a Debye curve with decreasing temperature below T_c in agreement with x-ray measurements. We show in table 1 the atomic arrangement and local symmetries above and below the ordering temperature. Because of the loss of symmetry associated with the rhombohedral distortion, the

16d site splits into two inequivalent sites 1b and 3d. The Mn atoms whose moments propagate with the vector $[\frac{1}{2}\frac{1}{2}\frac{1}{2}]$ belong to the 1b site. The magnetic structure can be then considered as a non-collinear, i.e. a ferrimagnetic canted structure. The crystallographic and magnetic parameters obtained from the Rietveld refinement at different temperatures are listed in table 2. Good agreement is obtained at each temperature between observation and calculation; the magnetic and crystallographic reliability factors are between 5 and 7%. The magnetic structure deduced is presented in figure 7.

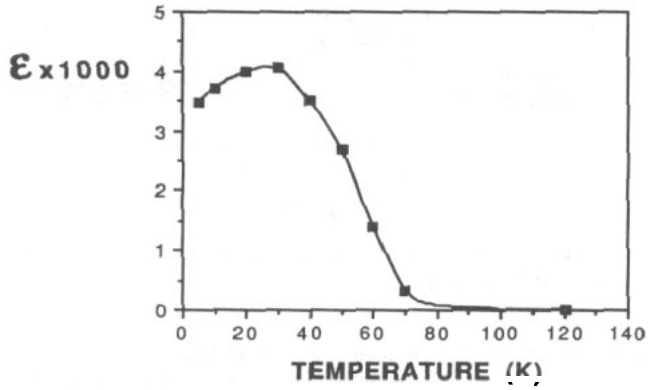

Figure 6. Thermal variation in the rhombohedral distortion parameter $\epsilon = 90 - \alpha_R$ for $Tb(Mn_{0.96}Fe_{0.04})_2$.

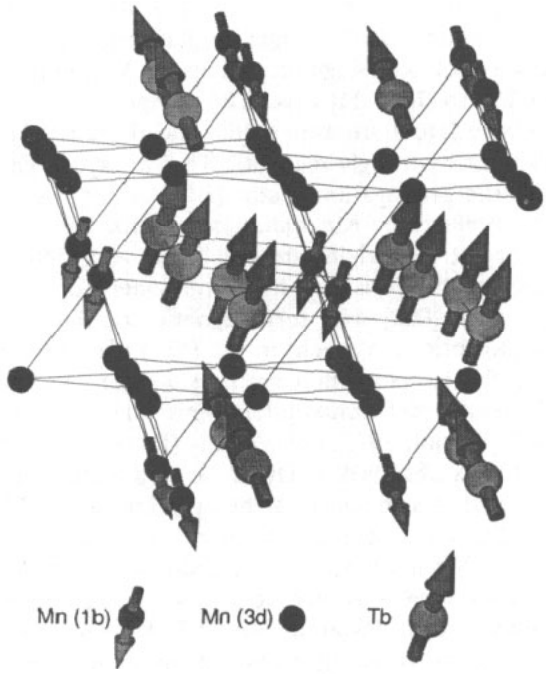

Figure 7. Magnetic structure of $Tb(Mn_{0.96}Fe_{0.04})_2$ below 30 K and the S_2 type structure of $TbMn_2$.

4. Discussion

The neutron diffraction experiments made on the $TbMn_2$ single crystal have shown clearly that the magnetic structure at 25 K under an applied field of 6.5 T is the same as $Tb(Mn_{0.96}Fe_{0.04})_2$, indicating the effect of external parameters on the stability of the Mn magnetism in $TbMn_2$. This magnetic structure is also stabilized by an applied hydrostatic pressure of 3.4 kbar (Mondal *et al* 1991). The same kind of spin structure is observed in $DyMn_2$ where the magnetism of Mn is destabilized. The rare-earth magnetism accounts for the stability of such a spin structure through Tb–Tb and Tb–Mn exchange interaction and the crystal-field effects. The crystal-field effects on the 4f shell of the Tb^{3+} ion are at the origin of the magnetic anisotropy and the large rhombohedral distortion. As in RFe_2 (Gignoux *et al* 1975) and RCo_2 (Gignoux *et al* 1979) this crystal distortion is strongly dependent on the magnetization direction. This behaviour has been discussed theoretically by Cullen and Clark (1977) in RM_2 Laves phases with M ≡ Fe, Co, Ni.

Table 1. Crystallographic parameters and space group of $Tb(Mn_{0.96}Fe_{0.04})_2$ above and below the ordering temperature.

Room-temperature phase, $Fd\bar{3}m$				Low-temperature ($T < 90$ K) phase $R\bar{3}m$			
Atom	Position		site symmetry	Atom	Position		Site symmetry
Tb	8a	$\frac{1}{8}\frac{1}{8}\frac{1}{8}$		Tb	2c	xxx	$3m$
		$\frac{7}{8}\frac{7}{8}\frac{7}{8}$	$\bar{4}3m$			$\bar{x}\bar{x}\bar{x}$	
Mn	16d	$\frac{1}{2}\frac{1}{2}\frac{1}{2}$		Mn	1b	$\frac{1}{2}\frac{1}{2}\frac{1}{2}$	$\bar{3}m$
		$\frac{1}{4}\frac{1}{4}\frac{1}{4}$					
		$\frac{1}{4}\frac{1}{4}\frac{1}{2}$	$\bar{3}m$		3d	$\frac{1}{2}00$	
		$\frac{1}{2}\frac{1}{4}\frac{1}{4}$				$0\frac{1}{2}0$	$2/m$
						$00\frac{1}{2}$	

The magnetic decoupling of Mn moments (1b and 3d) can be interpreted through the molecular field acting on these two sites. Indeed the molecular field resulting from the antiferromagnetic component of the neighbouring Tb moments vanishes on the Mn 3d site, and it is maximum on the 1b site. However, the molecular field resulting from the ferromagnetic component of Tb is the same at both sites. Different values of Mn moments are then expected. There are two possible arrangements of the ferrimagnetic Mn moments which give the same intensities for powder diffraction: either both sites 1b and 3d are magnetic with moments of $0.3\mu_B$ on each site, or only the 1b site is magnetic in which case the Mn(1b) moment is $1.37\mu_B$ at 5 K. The value of the Tb moment at 5 K is $8.70\mu_B$ in both cases. The magnetic moment of the Mn atoms at the 1b site cannot be induced directly by the local field due to terbium since in that case their directions should be parallel to the c axis which is the easy axis of magnetization for terbium. The fact that the antiferromagnetic components of moment are perpendicular to this direction indicates that a more complex process stabilizes the manganese moment (Ballou *et al* 1991c).

Owing to the similarity of the magnetic structure of $Tb(Mn_{0.96}Fe_{0.04})_2$ to that of $DyMn_2$ we think that only the 1b site is magnetic. In $DyMn_2$ (Yoshimura *et al* 1986a) the zero-field NMR spectrum, shows two peaks at 73 and 25 kHZ at 4.2 K. The higher-frequency peak is associated with a small fraction (25%) of Mn atoms

Table 2. Results of the Rietveld refinement of the crystallographic and magnetic parameters of neutron data of $Tb(Mn_{0.96}Fe_{0.04})_2$. The Mn–Mn distance can be obtained from the lattice parameter a by $d_{Mn-Mn} = a\sqrt{2}/4$.

			Tb moment			Mn moment					
						M_{ferro} (μ_B)		$M_{antiferro}$ (μ_B)		M (μ_B)	
T (K)	a (Å)	$\epsilon \times 10^3$ (rad)	M_{ferro} (μ_B)	$M_{antiferro}$ (μ_B)	M (μ_B)	1b	3d	1b	3d	1b	3d
120	7.5762	0	—	—	—	—	—	—	—	—	
70	7.5642	0.33	3.2	—	3.2	0.1	0.1	—	—	0.1	0.1
60	7.5595	1.4	5.08	—	5.08	0.13	0.13	—	—	0.13	0.13
						0.52	0	—	—	0.52	0
50	7.5547	2.7	6.5	—	6.5	0.15	0.15	—	—	0.15	0.15
						0.6	0	—	—	0.6	0
40	7.5508	3.5	7.37	—	7.37	0.2	0.2	—	—	0.2	0.2
						0.8	0	—	—	0.8	0
30	7.5477	4.05	8.14	—	8.14	0.22	0.22	—	—	0.22	0.22
						0.88	0	—	—	0.88	0
20	7.5436	3.98	8.42	1.28	8.52	0.22	0.22	0.2	0	0.28	0.22
						0.98	0	0.2	0	1.0	0
10	7.5412	3.70	8.37	2.38	8.70	0.25	0.27	0.63	0	0.67	0.27
						1.05	0	0.63	0	1.23	0
5	7.5407	3.49	8.32	2.53	8.70	0.3	0.3	0.66	0	0.72	0.3
						1.2	0	0.66	0	1.37	0

and the lower peak corresponds to the field transferred from Dy moments, implying almost no moment on the remaining Mn atoms. The cancellation of the moment at the 3d site is a common feature of manganese compounds such as $DyMn_2$ (Ritter *et al* 1991), $ThMn_2$ (Deportes *et al* 1987) and Mn_5Si_3 (Lander *et al* 1967) associated with the instability of Mn moments in frustrated lattices.

In contrast with $Tb(Mn_{0.96}Fe_{0.04})_2$, no spin rotation in the ordered state is observed in the TbM_2 compounds with M ≡ Fe, Ni and Co (Gignoux *et al* 1975, 1979). This shows that the magnetization direction of the Tb moment in all these compounds is [111]. The rotation observed in $Tb(Mn_{0.96}Fe_{0.04})_2$ must result from the Mn (1b) magnetic anisotropy. As in $NdMn_2$ (Ballou *et al* 1988) this anisotropy is associated with the strong uniaxial character of the local symmetry at the 1b site.

References

Ballou R, Brown P J, Deportes J, Markosyan A S and Ouladdiaf B 1991a *Proc. Int. Conf. on Magnetism (Edinburgh, 1991)*

Ballou R, Deportes J, Lemaire R, Nakamura Y and Ouladdiaf B 1987 *J. Magn. Magn. Mater.* **70** 129

Ballou R, Deportes J, Lemaire R and Ouladdiaf B 1988 *J. Appl. Phys.* **63** 3487

Ballou R, Gaydukova Y U, Markosyan A S and Ouladdiaf B 1991b *Proc. Int. Conf. on Magnetism (Edinburgh, 1991)*

Ballou R, Lacroix C and Nunez Regueiro M D 1991c *Phys. Rev. Lett.* **66** 1910

Bertaut E F 1972 *Ann. Phys., Paris* **7** 203

Chamberlain R 1977 *Physica* B **86–8** 138

Corliss M and Hastings J M 1964 *J. Appl. Phys.* **35** 1051

Cullen R and Clark A E 1977 *Phys. Rev.* B **15** 4510

Deportes J, Lemaire R, Ouladdiaf B, Roudault P and Sayetat F 1987 *J. Magn. Magn. Mater.* **70** 191

Felcher G P, Corliss L M and Hastings L M 1965 *J. Appl. Phys.* **36** 1001

Gignoux D, Givord F and Lemaire R 1975 *Phys. Rev.* B **12** 3878
Gignoux D, Givord F, Perrier De La Bathie R and Sayet F 1979 *J. Phys. F: Met. Phys.* **9** 763
Lander G H, Brown P J and Forsyth J B 1967 *Proc. Phys. Soc.* **91** 332
Levitin R Z, Markosyan A S and Pirogov A N 1988 *Sov. Phys.–JETP* **67** 2522
Mondal S, Cywinski R, Kilcone S H, Raiford B D and Ritter C 1991 *Proc. Int. Conf. on NS (Oxford, 27–30 August 1991)*
Ritter C, Kilcoyne S H and Cywinski R 1991 *J. Phys.: Condens. Matter* **3** 727
Shiga M 1988 *Physica* B **149** 249
Voiron J, Ballou R, Deportes J, Galera R M and Lelievre E 1990 *J. Appl. Phys.* **69** 5678
Wada H, Nakamura H, Fukami E, Yoshimura K, Shiga M and Nakamura Y 1987a *J. Magn. Magn. Mater.* **70** 17
Wada H, Nakamura H, Yoshimura K, Shiga M and Nakamura Y 1987b *J. Magn. Magn. Mater.* **70** 134
Yoshimura K, Shiga M and Nakamura Y 1986a *J. Phys. Soc. Japan* **55** 3585
Yoshimura K, Takigawa M, Yasuoka H, Shiga M and Nakamura Y 1986b *J. Magn. Magn. Mater.* **54–7** 1075